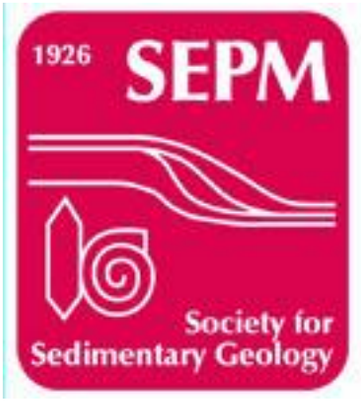

PALAIOS
Emphasizing the impact of life on Earth's history

PALAIOS, 2006, v. 21, p. 499–506
Research Note
DOI: 10.2110/palo.2005.P05-077R

EXPERIMENTAL PYRITE FORMATION ASSOCIATED WITH DECAY OF PLANT MATERIAL

FIONA BROCK,[1] R. JOHN PARKES[2] and DEREK E.G. BRIGGS[3]*

[1] *Research Laboratory for Archaeology and the History of Art, University of Oxford, Dyson Perrins Building, South Parks Road, Oxford, OX1 3QY, UK;*
[2] *School of Earth, Ocean and Planetary Sciences, Cardiff University, Main Building, Park Place, Cardiff, CF10 3YE, UK;*
[3] *Department of Geology and Geophysics, Yale University, P.O. Box 208109, New Haven, CT 06520-8109, USA*
e-mail: derek.briggs@yale.edu

ABSTRACT

Laboratory experiments on microbial decay were used to investigate the conditions required for pyritization of decaying twigs, as it provides an important source of data on the anatomy of fossil plants. Plane (*Platanus acerifolia*) was chosen as the experimental taxon, because this genus is preserved in pyrite in the Eocene London Clay. Experiments were designed to develop sulfate reduction under marine conditions, and each contained estuarine sediment with added iron oxide (1%) with a layer of pH-buffered artificial seawater medium above, which had a labile organic-matter source (yeast extract) and an inoculum of anaerobic, sulfate-reducing bacteria. Twigs (5) were pressed into the sediment and the systems incubated with a loose lid, in air at 15°C for up to 12 weeks. These conditions were varied to reflect those thought to promote pyrite formation in the natural environment (high concentrations of reactive iron and bioavailable organic matter, local concentration of decaying material, concurrent high concentrations of sulfide and iron, and oxidation of iron sulfides), plus variations in incubation time, anoxia, pH, and sulfate supply. Changes in the chemistry of the decay systems were monitored with oxygen and pH microelectrodes, and concentrations of sulfate, sulfide, ferrous iron, and sedimentary solid-phase sulfide pools were analyzed at the end of each experiment. All systems rapidly developed bacterial sulfate reduction, dissolved iron, and iron sulfides. In only 2 out of 18 reference systems were areas of some twigs pyritized, however, although this did occur rapidly (5.4 weeks). No twigs in the modified systems were pyritized despite up to a 240% increase in solid-phase iron sulfides, the presence of diffusion gradients of ferrous iron and sulfide, the focus of sulfate reduction on the twigs, and pyrite formation in the sediment. Neither slightly oxidizing nor completely anoxic conditions enhanced pyritization. These results suggest that conditions that promote formation of sedimentary pyrite differ considerably from those that facilitate pyritization of twigs. Pyritization can occur rapidly in conditions common in marine sediments with intense microbial activity, but the process is rather random and may be controlled by the nucleation of pyrite on decaying tissue rather than factors controlling pyrite formation.

INTRODUCTION

Here we describe laboratory model, microbial-decay experiments conducted to investigate the major factors considered to be important in determining the rapid pyritization of twigs. Fossil material provides only limited evidence for the processes involved in the authigenic mineralization of organic remains (e.g., Briggs, 1995, 2003). Experiments on microbial decay, however, can facilitate the study of soft-tissue mineralization and the factors that control it, including the relative influence of biological and abiotic processes (e.g., Sagemann et al., 1999; Grimes et al., 2001; Martin et al., 2003). While the fossilization of invertebrate soft tissues has been investigated experimentally (see Briggs, 1995), experiments on plant material have been more limited, focusing mainly on transport dynamics (e.g., Ferguson, 1985; Spicer, 1991), the role of bacterial biofilms (Dunn et al., 1997), and molecular taphonomy (e.g., Gupta et al., 2006).

Pyritized plant fossils are well documented from the Eocene London Clay of southeastern England, one of the best-preserved and most diverse fossil-plant assemblages in Europe (e.g., Bowerbank, 1840; Reid and Chandler, 1933; Chandler, 1964; Collinson, 1983; Poole, 1992). In the London Clay at the Isle of Sheppey, fossil twigs and roots have revealed relationships between cell type, pyrite textures, and quality of preservation (Grimes et al., 2002), but even here plant material is incompletely pyritized (Allison, 1988; Grimes et al., 2002). Other London Clay fossil sites show much less pyritization (M.E. Collinson, personal communication, 2005).

Plant tissues are susceptible to decay and usually are degraded completely, but under certain conditions they are preserved as organic fossils or by authigenic mineralization (Schopf, 1975; Scott, 1990). One of the most important minerals involved in the fossilization of soft tissues, including plants, is pyrite (Scott, 1990). They are found notably at such sites as Chengjiang in the Lower Cambrian of Yunnan Province, China (Gabbott et al., 2004), Beecher's Trilobite Bed in the Upper Ordovician of New York State (e.g., Briggs et al., 1991) and the Lower Devonian Hunsrück Slate of western Germany (e.g., Briggs et al., 1996; Bartels et al., 1998), and sparsely at such sites as the Middle Cambrian Burgess Shale of British Columbia (e.g., Conway Morris, 1986) and the Jurassic of La Voulte-sur-Rhône in France (Wilby et al., 1996). Although there are limited examples in the fossil record, the preserved material can provide valuable information about the organisms preserved as well as the depositional environmental conditions. Poor understanding of the processes involved in and conditions required for soft-tissue pyritization, however, limit our interpretation of the fossil record of pyrite.

Pyritization of plant material within a lithology is often patchy; pyrite may preserve just part of the plant (e.g., the central strand of an otherwise coalified axis) and may be oxidized to limonite, which pseudomorphs the original textures (Kenrick et al., 1991). Pyritized plant fossils are nonetheless the most common source of data on the three-dimensional anatomy of early vascular plants (Kenrick and Edwards, 1988; Kenrick et al., 1991), facilitating the analysis and interpretation of cell-wall ultrastructure and providing data on the evolution of water-conducting tissues and the diversification of vascular land plants during the Devonian (Kenrick and Edwards, 1988; Friedmann and Cook, 2000).

Pyrite is considered generally to be a product of the reaction of bacterially produced hydrogen sulfide with reactive detrital iron minerals in sediment. These produce a series of metastable iron monosulfides such as mackinawite, amorphous FeS, and greigite (Berner, 1970), which are then converted to pyrite. In addition to the direct reaction of detrital iron minerals with hydrogen sulfide (Sørensen, 1982; Canfield, 1989a; equation 1), there are several important reactions that produce the precursors of iron monosulfides (Canfield and Raiswell, 1991), including reduction of iron minerals by dissimilatory iron-reducing bacteria (e.g., Sørensen,

* Corresponding author.

 0883-1351/06/0021-0499/$3.00

1982; Lovley and Philips, 1986a, 1986b; Canfield, 1989b; equation 2) and ferrous iron formation by the partial oxidation of iron sulfide minerals (Aller, 1980; Giblin and Howarth, 1984; equation 3) prior to reaction with hydrogen sulfide (equation 4).

$$2FeOOH + H_2S + 4H^+ \rightarrow 2Fe^{2+} + S^0 + 4H_2O \quad (1)$$

$$4FeOOH + CH_2O + 8H^+ \rightarrow 4Fe^{2+} + CO_2 + 7H_2O \quad (2)$$

$$2FeS_2 + 7O_2 + 2H_2O \rightarrow 2Fe^{2+} + 4SO_4^{2-} + 4H^+ \quad (3)$$

$$Fe^{2+} + H_2S \rightarrow FeS + 2H^+ \quad (4)$$

Iron monosulfides transform readily to pyrite during early diagenesis, but the processes involved are not understood properly; the range of geochemical environments in which pyrite is found, and its ubiquity in modern sediments and ancient sedimentary rocks, suggest that multiple pathways may be involved. The transformation of iron monosulfides to pyrite has been proposed to occur via polysulfides or aqueous sulfur (Berner, 1969; Benning et al., 2000), H_2S (e.g., Drobner et al., 1990; Rickard, 1997; Butler and Rickard, 2000), or sulfur oxyanions (Schoonen and Barnes, 1991b). Wilkin and Barnes (1996) suggested that O_2, H_2O_2, Fe(III), Mn(VI, III), nitrate, organic carbon, and bicarbonate could all be important oxidants in the formation of pyrite in sedimentary environments. Pyrite forms naturally under marine conditions with a range of pH 6–9 (Stumm and Morgan, 1981) and in the laboratory between pH 5.5 and 8 (e.g., Berner, 1969; Luther, 1991; Rickard, 1994; Wilkin and Barnes, 1996).

In normal marine conditions where bottom waters are oxygenated, the major factors influencing the rate of bacterial sulfate reduction, and hence pyrite formation, are the amount and reactivity of available organic matter (Berner, 1984) and iron (Berner, 1984; Raiswell and Canfield, 1988). The overall reactivity of organic matter decreases during decomposition as the more reactive compounds are consumed. Degradation of the remaining, less reactive compounds, and any geopolymers formed by aging, results in subsequently lower rates of sulfate reduction (Berner, 1984) and hence potentially less pyrite formation.

Regardless of the depositional environment, the amount of pyrite formed is almost never limited by the total amount of iron present (Berner, 1984), but it is strongly influenced by the reactivity of iron. There is a suite of sedimentary iron minerals ranging in reactivity from iron oxides, which react rapidly with dissolved sulfide (fastest half life 2.8 hr), to iron-bearing silicates, which react much more slowly (84,000 years: Canfield, 1989b; Canfield et al., 1992; Raiswell and Canfield, 1988). Sulfate concentration is high in marine conditions where most pyrite is formed (Kaplan et al., 1963), and here its effect on pyrite formation may be relatively unimportant. In freshwater environments, however, where concentrations of dissolved sulfate are two orders of magnitude lower, sulfate concentrations are a major controlling factor and little pyrite forms (Berner, 1984).

Plant cells do not contain enough metabolizable material to produce sufficient pyrite to infill the cell completely (Grimes et al., 2001). Oxidation of iron monosulfide by hydrogen sulfide, however, produces hydrogen (Drobner et al., 1990), which can be used as a substrate by some sulfate-reducing bacteria (Widdel and Bak, 1992) that potentially lead to additional pyrite formation. Even where this occurs, however, pyritization of organic matter may be limited by the rate of transport of iron and sulfur into the cell and by the rate of pyrite nucleation (Schoonen and Barnes, 1991a; Raiswell, 1993; Grimes et al., 2001; Allen, 2002). Raiswell et al. (1993) proposed a three-dimensional model of diffusion-with-precipitation to explain the preservation of animal carcasses, demonstrating the requirement for unusually high porewater-dissolved iron to confine precipitation of iron sulfide to the decay site. Nonetheless, despite requiring specific depositional conditions (Briggs et al., 1991; Raiswell et al., 1993), pyritization of plants is relatively common, if locally developed, in marine settings (Spicer, 1991).

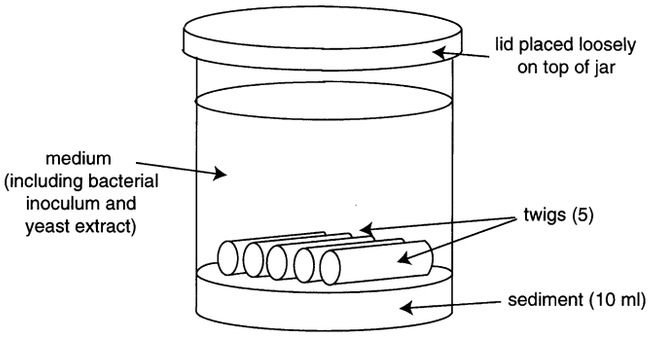

FIGURE 1—Setup used to conduct the experiments.

METHODS

Plane (*Platanus acerifolia*) was chosen as the main experimental taxon, because the genus is preserved in pyrite in the Eocene London Clay (Poole, 1992; Poole et al., 2002). The role of such different factors in pyritization as concentration and reactivity of iron and organic matter, sulfide concentration, oxidation of iron sulfides, pH, and sulfate supply was investigated by varying experimental conditions. The results were compared to those obtained under reference marine conditions set up as follows (Fig. 1): Amorphous iron oxyhydroxide (FeOOH), one of the detrital iron minerals most reactive to sulfide (Canfield et al., 1992), was prepared (Lovley and Philips 1986b), mixed thoroughly (1% wt) with fresh anoxic sediment (10 ml) from an estuarine site with local plant input (banks of the River Wye, Chepstow, UK), and spread into an even layer covering the base of a 100 ml wide-necked screw-top glass jar. Five fresh, 1–2 year old plane twigs 35–40 mm in length and of similar mass, with no visible knots, decay, or damage, were placed in a single layer and pressed slightly into the sediment. Seven ml of yeast extract solution (1.5%) was added as an extra energy source to encourage bacterial growth, followed by a bacterial inoculum (10 ml). This inoculum contained a mixed anaerobic sulfate-reducing bacterial community that was cultured from the same sediment in an anaerobic sulfate-reducing bacterial medium (Widdel and Bak, 1992) with homogenized plane twigs. The bacterial inoculum and readily degradable yeast extract were used as these conditions produced steep chemical gradients considered important in fossilization (Sagemann et al., 1999). The total volume in the jar was made up to 100 ml with artificial seawater similar to that of Widdel and Bak (1992), containing (g/l): NaCl, 20.0; $MgCl_2 \cdot 6H_2O$, 3.0; KCl, 0.5; NH_4Cl, 0.25; KH_2PO_4, 0.20; $CaCl_2 \cdot 2H_2O$, 0.15; Na_2SO_4, 4.0. After autoclaving, the medium was cooled under N_2/CO_2, set to pH 7.5 with 2M NaOH. A reduced amount of bicarbonate buffer solution was added (0.005%) to approximate marine sediment buffer capacity (Sagemann et al., 1999). An unlined polypropylene lid was used to minimize evaporation and provide cover, while allowing gaseous diffusion. Jars were incubated in a waterbath at 15°C in natural daylight.

Decay experiments were conducted for up to 12 weeks, because preliminary experiments indicated that elevated bacterial activity usually was sustained for this time. After this time, oxygen concentrations increased and systems started to oxidize, reflecting a slowing of bacterial decay. Gradients of oxygen and pH were monitored every 2–3 days directly above the twigs on a submillimeter scale using microelectrodes (Diamond General, Ann Arbor, USA) to determine chemical gradients with minimum disturbance to the decay environment (see Sagemann et al., 1999). At the end of each experiment aqueous samples were removed from just below the air–medium interface and just above the sediment–medium interface. Samples were stored as follows: 1 ml in 10% (w/v) zinc acetate solution each for sulfide and sulfate analysis; 1 ml in 0.5M HCl for analysis of dissolved Fe (II). Sulfide concentrations were measured colorimetrically (Cline, 1969). Samples were treated with an equal volume of 1:1 mixture of acidified ferrous chloride solution (60 g per liter 50% HCl) and N,N-dimethyl-p-phenylene diamine solution (40 g per liter 50%

HCl) for 50 minutes before being diluted 5 times with deionized water. After a further 5 minutes, color intensity was measured spectrophotometrically at 670 nm, and molarity was calculated by comparison with a range of standards. Sulfate was analyzed by ion chromatography (Dionex Inc.). Ferrous iron was measured using the method of Stookey (1970). Samples (0.5 ml) were treated with ferrozine solution (5 ml, 0.5 g ferrozine dissolved in 500 ml of 50 mM HEPES buffer at pH 7.0). The color was allowed to develop for 30 minutes before color intensity was measured spectrophotometrically at 562 nm, and molarity was calculated by comparison with standards.

Sediment-sulfide pools were separated into three H_2S fractions (acid volatile sulfide, pyritic sulfide, and elemental sulfur) by a sequential distillation of cold followed by hot chromous chloride digestions (following Allen and Parkes, 1995). Sediment samples were treated with 6M HCl (2 ml) and distilled at 80°C for 40 minutes for the AVS fraction. After cooling, the sediment was treated with 95% ethanol (5 ml), chromous chloride (25 ml), and concentrated HCl (5 ml) and distilled for 40 minutes for the pyritic sulfide fraction. The sediment was then heated to 80°C for a further 40 minutes for the elemental sulfur fraction. The sulfide in each fraction was collected in 10 ml 10% zinc acetate solution and measured spectrophotometrically (as above) and the total reduced inorganic sulfur (TRIS) was calculated as the sum of all three fractions in each sample.

Scanning electron microscopy (SEM) was used to study changes in tissue structure caused by decay and to monitor the growth of minerals within the plant material. On removal from the decay systems, twigs for SEM analysis were fixed in 95% ethanol/acetic acid (3:1) before being taken through an ethanol dehydration series (15%, 30%, 50%, 70% for 30 minutes each). The twigs were cut into 2-mm-thick sections that were taken through a further ethanol dehydration series (95%, 100%, 100% for 1 hour each) before being immersed in hexamethyldisilizane (HMDS) for 1 hour. Sections were mounted on aluminum stubs and coated with gold for secondary electron imaging, or carbon for backscatter imaging, on a Cambridge Stereoscan 250 Mk3 SEM. Minerals were identified using an Oxford Instruments PCXA energy-dispersive analyzer (EDS).

Investigation of the Effect of Environmental Variables on Plant Pyritization

Continuing Sulfate Supply.—A 5% agar layer (10 ml) of sodium sulfate (30 mM) was placed underneath the sediment. Initial tests demonstrated that sulfate was released into the overlying medium for up to 10 weeks.

Concentrations of Iron and Reactive Iron.—Experiments were conducted with additional reactive iron oxyhydroxide (3% and 5% wt). Hematite and hematite–FeOOH and ferric chloride–FeOOH mixtures were used as alternative (1%) iron sources with different reactivity for microbial iron reduction and to hydrogen sulfide.

Increase in Concentrations of Labile and Recalcitrant Organic Matter.—Because plants contain insufficient metabolizable material for complete pyritization, soluble glucose (20 mM) was added to reference decay systems after six weeks of incubation in order to stimulate bacterial activity, including sulfate reduction. The effect of additional recalcitrant organic matter was investigated in separate experiments by varying the number of twigs (1, 5, and 15).

pH.—Because some initial experiments had shown pyritization under slightly lower maximum pH conditions (see section on results, below), 1% $FeCl_3$ was used as an alternative iron source to FeOOH to decrease pH. Because this did not significantly reduce the pH of the medium, however, these experiments were repeated with drop-wise addition of HCl (50%) reducing pH to 6.5–7.0 every 2–3 days.

Pyritization under Anoxic Conditions.—If pyritization is due to H_2S as an oxidizing agent (Rickard, 1997), then pyritization will be enhanced under anoxic conditions. Reference systems were set up under anaerobic conditions in 100 ml Duran bottles sealed with a PTFE (polytetrafluoroethylene) bung and O-ring-sealed screw cap. These bottles were stored in clear anaerobic gas bags flushed with N_2/CO_2 (80:20) in the dark at 15°C.

RESULTS

Concentrations quoted in the text are mean values from replicates in Table 1.

Standard Marine Reference System

Four different experimental runs were conducted (Table 1), each with their own reference marine systems for direct comparison. All reference systems developed very similarly. Experiment 1 is described in detail, because it involved a comprehensive time course, with destructive sampling and analysis of one jar per week (week 0 denotes the starting conditions). Most other comparisons are based on 12-week incubations (Table 1).

Initial rapid bacterial activity maintained anoxia below the top few millimeters of the medium for the first 3–4 weeks. This was accompanied by a rapid decrease in sulfate concentration (29.5 to 16.7 mM), increase in sulfide (0.28 mM), blackening of the sediment, and an increase in all forms of solid-phase sedimentary sulfide pools, and thus TRIS (3.2 mM; Fig. 2). This intense sulfate reduction slowed after week 2 as sulfate removal rates and solid phase sulfide formation slowed. By week 5, oxygen penetration increased and dissolved sulfide decreased to nearly zero, although there was still a low rate of sulfate removal and a slow increase in TRIS. By about week 9 a steady increase in sulfate, accompanied by an overall decrease in TRIS, demonstrated a change in redox conditions and a shift to sulfide oxidation (Fig. 2). As decay intensity continued to decrease with time, oxygen penetrated to greater depths within the aqueous medium, although the sediment and the medium immediately above it remained anoxic for the duration of the experiment (Figs. 1 and 2).

There were some surprisingly large and erratic pH changes through time. The pH of the medium dropped initially from 7.5 to 6.5 (data not shown) before rising to 7.9 by week 1. The pH then continued to rise, reaching a maximum of 9.8 after week 6, and then decreased erratically to 8.6 after week 12. The periods of pH increase and decrease broadly coincided with the periods of sulfate reduction and sulfide oxidation, respectively.

SEM analysis of the twigs from reference experiments revealed precipitation of iron sulfide (FeS and FeS_2) along the cell walls and within the cells of several twigs in just 2 out of 18 marine replicates incubated longer than 5 weeks (Fig. 3). These two systems were both from Experiment 2, and FeS/FeS_2 was formed by week 5.4 and was still present at week 12. Slightly higher sulfide was present at the sediment-medium interface after 5.4 weeks compared to reference systems in Experiment 1, and the pH maximum was lower (pH 8.6, Table 1) than in other reference systems. Hence, pH was lowered in some subsequent experiments.

Effect of Sulfate Availability

Slow release of sulfate into the decay system resulted in higher sedimentary TRIS (3.8 mM) and higher sulfide (0.2 mM) at the sediment-medium interface than in reference marine systems (Table 1, Experiment 3). Black iron monosulfide (AVS) Liesegang bands formed within the agar layer (see Allen, 2002).

Effect of Iron Availability: Amount of Iron Oxyhydroxide Added to the Sediment

Systems with 3% and 5% FeOOH also had higher sedimentary TRIS (3.6 mM), and the 3% FeOOH system had slightly higher sulfide (0.06 mM) at the sediment-medium interface than in reference marine systems (Table 1, Experiment 3). Higher FeOOH concentrations, however, did not result in an increase in concentrations of dissolved ferrous iron.

TABLE 1—Concentrations of sulfate, sulfide, and ferrous iron within the medium adjacent to the decaying plant material and the corresponding sedimentary sulfide pools after decay. Standard open marine systems were run alongside each experiment. The two marine systems in which amorphous FeS formed within the plant tissues were not run alongside any other experiments and are labeled (FeS_{am}); — denotes no data available.

Experimental conditions	Weeks	Sulfate (mM)	Sulfide (mM)	Fe (II) (mM)	AVS (mM)	Pyritic S (mM)	S° (mM)	TRIS (mM)
	Experiment 1							
Standard marine reference system	0	29.5	0	0.01	0	0.6	0.1	0.7
Standard marine reference system	1	22.1	0.15	0.20	0.2	0.8	0.3	1.3
Standard marine reference system	2	174	0.40	0.05	1.2	1.5	0.4	3.0
Standard marine reference system	3	16.7	0.28	0	0.9	1.4	0.9	3.2
Standard marine reference system	4	14.7	0.30	0	1.0	1.5	0.4	2.8
Standard marine reference system	5	8.9	0.01	0.02	1.2	1.6	0.4	3.3
Standard marine reference system	6	15.7	0.02	0.01	1.3	1.7	0.5	3.5
Standard marine reference system	7	12.9	0.02	0.01	1.1	1.6	0.4	3.1
Standard marine reference system	8	16.4	0	0	1.1	1.7	1.0	3.7
Standard marine reference system	9	11.0	0.05	0	1.8	1.6	1.1	4.6
Standard marine reference system	10	16.8	0	0	1.3	1.7	0.5	3.4
Standard marine reference system	11	10.6	0	0	1.3	1.0	0.9	3.1
Standard marine reference system	12	14.2	0	0	1.0	1.5	0.9	3.4
Organic matter availability: + glucose	12	10.7	0	0	2.1	1.6	0.7	4.4
Organic matter availability: + glucose	12	7.1	0	0	1.6	1.9	0.7	4.2
Effect of pH: $FeCl_3$ + HCl	12	2.5	0	0	1.5	1.5	0.7	3.7
Effect of pH: $FeCl_3$ + HCl	12	3.2	0	0	1.7	1.1	1.0	3.8
	Experiment 2							
Standard marine reference system (FeS/FeS_2 formed)	5.4	13.9	0.31	0.04	—	—	—	—
Standard marine reference system (FeS/FeS_2 formed)	12	14.1	0	0.03	—	—	—	—
	Experiment 3							
Fresh sediment	—	—	—	—	0.0	0.4	0.2	0.6
Standard marine reference system	12	21.2	0	0.02	1.3	1.0	0.6	2.9
Standard marine reference system	12	21.0	0.01	0.04	0.5	1.4	0.3	2.2
Sulfate availability: + SO_4^{2-} agar layer	12	14.4	0.01	0.05	1.6	1.8	0.7	4.1
Sulfate availability: + SO_4^{2-} agar layer	12	8.4	0.46	0.02	1.1	1.5	0.8	3.4
Iron availability: 5% FeOOH	12	15.1	0	0.02	—	—	—	—
Iron availability: 5% FeOOH	12	13.4	0	0.02	2.2	1.2	0.6	4.0
Iron availability: 3% FeOOH	12	17.4	0.03	0	1.3	1.8	0.6	3.6
Iron availability: 3% FeOOH	12	12.5	0.08	0	1.2	1.6	0.4	3.2
Iron reactivity: haematite	12	21.1	0	0.01	1.7	1.6	0.4	3.6
Iron reactivity: haematite	12	22.4	0	0.02	1.3	1.1	0.4	2.8
Iron reactivity: haematite/FeOOH	12	21.9	0	0.01	—	—	—	—
Iron reactivity: haematite/FeOOH	12	19.8	0	0.01	1.2	1.3	0.6	3.1
Iron reactivity: $FeCl_3$/FeOOH	12	17.8	0	0.01	2.6	2.3	0.5	5.3
Iron reactivity: $FeCl_3$/FeOOH	12	17.5	0	0.02	1.4	1.3	0.4	3.1
Organic matter availability: single twig	12	26.0	0	0.01	0.1	0.4	0.3	0.8
Organic matter availability: single twig	12	25.3	0	0	0.4	0.6	0.3	1.3
Organic matter availability: 15 twigs	12	4.6	0.13	0.04	2.3	1.6	0.4	4.3
Organic matter availability: 15 twigs	12	10.2	0.15	0.03	2.2	1.3	0.9	4.4
Effect of pH: $FeCl_3$	12	13.1	0	0.02	1.8	1.9	1.0	4.7
Effect of pH: $FeCl_3$	12	14.6	0	0.01	2.1	1.7	1.0	4.8
	Experiment 4							
Standard marine reference system	12	11.7	1.3	0	—	—	—	—
Standard marine reference system	12	12.3	1.3	0	—	—	—	—
Effect of eliminating oxygen	12	0	4.3	0	—	—	—	—
Effect of eliminating oxygen	12	0	6.9	0	—	—	—	—

Effect of Iron Reactivity

The use of different sedimentary iron sources resulted in variability in TRIS, sulfate concentrations, and oxygen saturation between replicate decay systems. TRIS and ferrous concentrations, however, were not consistently higher than in other treatments (Table 1, Experiment 3), although TRIS was higher (3.6 mM) than in parallel reference marine conditions (2.6 mM). Consistently less alkaline (by up to 0.5 units) was the pH in the mixed-iron systems than in the FeOOH reference systems. Sulfate concentrations were lower, and TRIS concentrations slightly higher (4.2 mM) in the ferric chloride–FeOOH systems.

Increase in Concentrations of Labile and Recalcitrant Organic Matter

Promoting Bacterial Activity with Glucose.—After 12 weeks of decay, sulfate concentrations were much lower at the sediment-medium interface than in the reference systems (8.9 and 14.2 mM, respectively: Experiment 1). TRIS and AVS concentrations were elevated similarly to those in treatments with additional twigs, iron, and $FeCl_3$/pH (TRIS 4.3 mM, Table 1).

Number of Twigs Added to Decay Systems.—Decay systems with a single twig were oxic after 12 weeks, with sedimentary TRIS concentrations similar to those of the fresh sediment (0.6 mM, Table 1, Experiment 3). In contrast, systems with 15 twigs remained anoxic at the sediment-

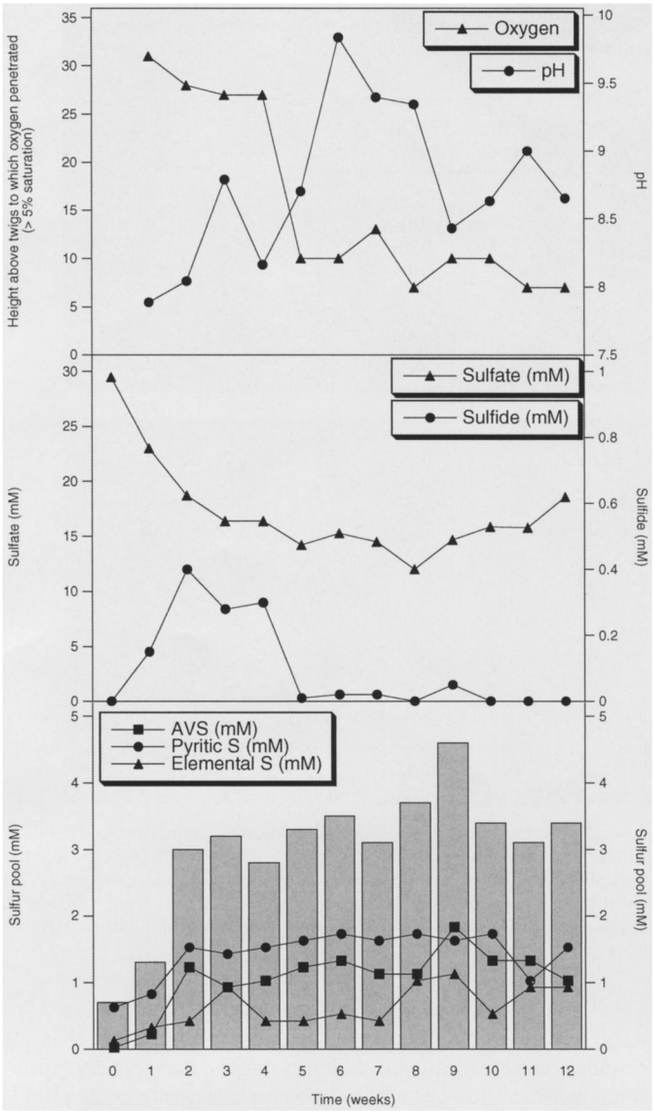

FIGURE 2—Changes in chemical composition of medium immediately adjacent to decaying plant material and sedimentary sulfide pools in open marine decay systems over 12 weeks. Histogram represents total reduced inorganic sulfur (TRIS) in the sediment.

medium interface after 12 weeks; sulfate concentrations were lower than in the reference systems; TRIS, and particularly AVS, were elevated (4.3 mM and 2.2 mM, respectively). The pH was also slightly less alkaline than in reference systems containing 5 twigs (pH 8.4–8.5 compared with pH 8.7–8.9, respectively).

Effect of pH

The use of ferric chloride as an iron source instead of iron oxyhydroxide to reduce pH resulted in the highest TRIS concentrations (4.7 mM) and low sulfate concentrations (Table 1, Experiment 3). The pH of the medium, however, was only 0.3 units lower than in the reference systems after 12 weeks (pH 8.6 compared to pH 8.8–8.9). In the ferric chloride systems to which HCl acid additions were made, the pH stabilized at 7.5–8.0 within 2–3 days of each addition, reflecting the buffer capacity of the medium. This resulted in enhanced sulfate reduction, with sulfate concentrations the lowest in any open system (2.9 mM). The iron sulfides that formed, however, did not accumulate on or within the sediment or plant material (TRIS concentrations 3.7 mM, only slightly higher than in reference systems; 3.4 mM; Table 1, Experiment 1), but remained as a grey to black suspension within the medium.

Effect of Anoxic Conditions

After 12 weeks of decay in the absence of oxygen, no sulfate was present and 5.6 mM of sulfide was measured at the medium-sediment interface, compared with ~1.3 mM sulfide and 12 mM sulfate in the reference systems (Table 1, Experiment 4). The sediment turned black, indicating the formation of AVS, although no data on solid-phase sulfide were available. In addition, after 12 weeks, the pH was 7.2 compared to 9.0 in the open reference system.

DISCUSSION

A mixture of FeS and FeS_2 formed at a cellular level within the plant material in just two of the reference marine decay systems (Fig. 3). None of the systems modified to explore the effect of potential variables controlling pyritization resulted in the formation of iron sulfides within the plant material. The rate of bacterial sulfate reduction, concentration of sulfide, concentration and type of sedimentary solid-phase sulfides, and pH, however, were influenced. In addition, where pyritization did occur, the formation of iron sulfide was rapid (Figs. 3A and 3B), underlining the intimate involvement of intense bacterial processes. Individual pyrite crystals were evident after only 5.4 weeks, and crystals occurred on the pith parenchyma cell walls, in the middle lamella, and at the junction of the cell walls after 12 weeks, infilling several pith cells in one case (Fig. 3B). Similar structures are preserved in pyritized twigs from the Eocene London Clay (Figs. 3C and 3D; Grimes et al., 2002).

TRIS was increased (up to 240%) under a range of conditions, including increased concentrations of reactive iron, mixed iron sources, $FeCl_3$, addition of glucose, and increased twig numbers (Table 1). Hence, iron sulfides were being formed in the sediment, but not within the twigs. This suggests that the conditions that control the formation of iron sulfides in sediment, including pyrite (Fig. 2), are different from those controlling plant pyritization. Both, however, depend on the availability of metabolizable tissue to promote sulfate reduction. Raiswell et al. (1993) considered that the diffusion of concentrations of high pore-water ferrous iron into a carcass where bacterial sulfate reduction was focused could explain pyritization of trilobites in Beecher's Trilobite Bed in the Ordovician of New York State.

The formation of Liesegang bands of AVS within the agar layers in the systems set up to investigate the role of sulfate availability demonstrated that diffusion of reactants for pyrite formation was occurring even though the twigs did not become pyritized. This situation also demonstrated that distributions of ferrous iron and sulfide were not homogeneous. Liesegang banding is a common occurrence in authigenic pyrite systems (Berner, 1969). Allen (2002) proposed that the formation of such discrete bands plays a role in the development of gaps between sites of organic-matter preservation and pyrite formation, providing a mechanism for the formation of pyrite halos, concretions, rims, and overgrowths. Allen (2002) also proposed that Liesegang banding indicates that a system is iron-limited. Iron, however, was probably not limiting in our systems, because increasing the iron concentration by a factor of 5 resulted in only a limited increase in TRIS. Even the reference 1% FeOOH (~100 mM) was in excess of the TRIS produced and sulfate reduced (max ~25 mM, 4.6 mM sulfate remained in one of the 15 twig systems in Experiment 3). In addition, the 3% and 5% FeOOH added to the experiments should have generated concentrations of dissolved iron greater than those predicted for either Beecher's Trilobite Bed (Briggs et al., 1991) or the Hunsrück Slate (Briggs et al., 1996), particularly because reactive FeOOH may be reduced in preference to sulfate by anaerobic bacteria (Lovley and Chapelle 1995). Once anoxic conditions developed in our experiments, reduction of bacterial ferric iron could have led initially to the production of ferrous ions, followed by sulfate reduction and sulfide formation (e.g., Experiment 1, week 1: ferrous 0.2 mM, sulfide 0.15 mM). Because initial

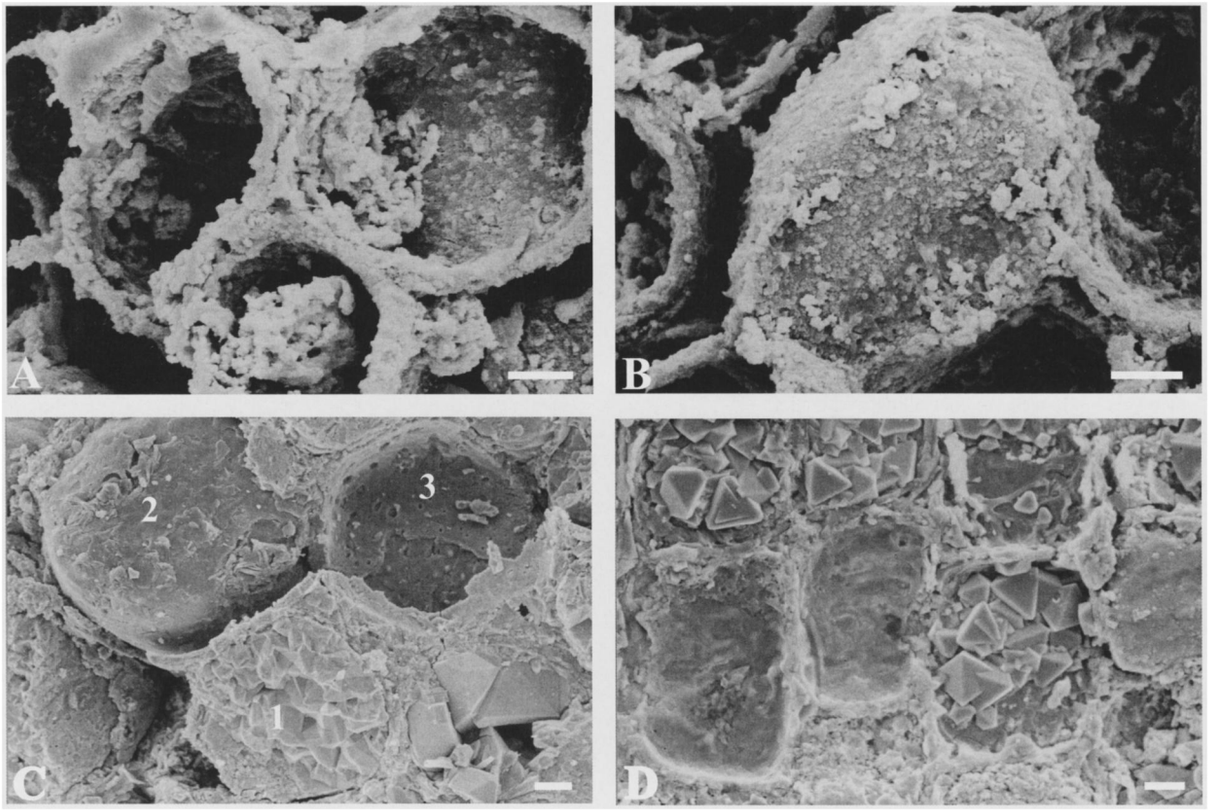

FIGURE 3—Comparison of experimentally induced plant pyritization with examples from the Eocene London Clay. (A, B) Secondary scanning electron microscope (SEM) images (Cambridge Instruments S360 SEM-WDS [wavelength-dispersive spectroscopy]) from microbiological pyritization experiments on plane twigs (*Platanus* sp.). (A) Different styles of experimental FeS and FeS_2 mineralization in general view of *Platanus* pith. (B) Extensive experimental mineralization of *Platanus* pith cell. (C, D) Pyritized fossil *Plataninium* counterparts from fracture sections from Eocene London Clay. (C) Pyritized fossil *Plataninium* pith cells filled with interlocking pyrite (cell 1), fine-grained pyrite generating cast of internal cell surface upon which grew framboidal and polycrystalline pyrite (cell 2) and pyritized cell wall with pits (cell 3). (D) Pyritized dicotyledonous root. Scale bars 10 μm. (Photographs reproduced, with permission, from Grimes et al., 2001).

bacterial activity would have utilized the most labile organic matter (e.g., yeast extract and sedimentary dissolved organic matter), sulfate reduction must have utilized the less labile twig tissue.

Increase in TRIS formation with number of twigs (1, 5 [reference system] and 15 twigs, Experiment 3, Table 1) confirmed that the twigs decayed even under the anoxic conditions that developed in these experiments, and would have been a focus for sulfate reduction. When completely anoxic systems were studied, all sulfate was reduced and high concentrations of sulfide (5.6 mM) persisted for 12 weeks. Under these conditions no ferrous iron diffused into the overlying medium (Table 1), and therefore, there would have been high concentrations of both sulfide and iron in the sediment. Surprisingly, however, no pyritization of the twigs was observed. Black AVS was also present and the pH was approximately neutral, conditions that should have been suitable for pyritization by H_2S oxidation of FeS (Rickard, 1997). Similarly, when oxygen penetrated close to AVS-containing sediment after about week 5 in the reference systems open to the atmosphere, pyritization would have been possible in these slightly oxidizing conditions via partly oxidized sulfur species (Schoonen and Barnes, 1991a, 1991b; Benning et al., 2000), if this were a rapid process. The steady increase in sulfate concentrations after about week 8 (Fig. 2) showed that oxidation of sulfides was occurring, and thus the presence of partially oxidized sulfur species was highly likely, but no pyritization occurred. There was a tendency for pyrite concentrations to decrease over time in these experiments (Table 1).

The reference marine systems developed surprisingly high pH values, reaching a maximum of pH 9.8 after 6 weeks but then declining to pH 8.6–8.8 after 12 weeks. Although pH rose steadily over 12 weeks in the two systems where the twigs were pyritized, however, it reached a maximum of only pH 8.6. It is unclear what caused the difference in pH conditions in these decay systems. It may reflect a change in decay pathways, bacterial activity or related geochemical reactions, or the pH difference may have resulted in the pyritization or been a consequence of it. In subsequent experiments with a lower pH (6.5–8.0) no pyritization occurred, suggesting that lower pH might not have been a direct cause of the pyritization in previous experiments. pH, however, clearly had an impact on iron sulfide formed in the systems, inasmuch as in the lower-pH controlled experiments FeS formed within the medium as opposed to the sediment or the plant material, and hence presumably was in the form of soluble FeS ($FeS_{(aq)}$ of Rickard and Luther, 1997).

CONCLUSIONS

These experiments investigated a range of conditions purported to be required for pyritization. None of these resulted in consistent pyritization. Instead, pyritization occurred, seemingly randomly, in two reference systems, albeit under conditions of slightly lower maximum pH (pH 8.6). In addition, both of these systems were part of the same experimental series (Experiment 2). This suggests that some subtle difference between these and other reference systems facilitated pyritization. Differences may have existed in the twigs (e.g., biochemical or cellular composition), the sediment used (microbial and geochemical composition and amount of organic matter present), or the bacterial inoculum (development of different dominant populations). Even in the successful experiments, however, iron sulfides only formed in small areas on the surface of the twigs and never on more than one twig from each system. This indicates that conditions required for pyritization of twigs were extremely local. This

may be related to the persistence of heterogeneous chemical and microbiological conditions in our experiments in spite of diffusion of soluble chemical species.

Another factor affecting pyritization is pyrite nucleation on the twig cells. Pyrite can be difficult to nucleate (Schoonen and Barnes, 1991a), although nucleation of iron monosulfides and pyrite has been reported on such organic surfaces as bacterial cell walls (Donald and Southam, 1999) and on and within the cell walls of celery (Grimes et al., 2001). Biochemical, geochemical, mineralogical, or microbial differences at or near the twig surfaces may have controlled pyritization via nucleation of the consistently formed TRIS. Unfortunately, our fragile microelectrodes could not be used at, or within, the twig surface to investigate microscale gradients and processes very close to the twig surface. Thus, we could not determine whether heterogeneous conditions influencing nucleation on the twig cells were a factor controlling pyritization.

Our results show that plant pyritization can occur within a few weeks to months, under conditions that are representative of those that commonly occur in marine sediments with intense microbial activity. Pyritization under these conditions, however, is a rather random process controlled by local conditions, probably including factors that influence nucleation. None of the conditions and variables purported to enhance pyritization of plant material promoted it in our experiments. These results are consistent with the occurrence and distribution of pyritized fossils in ancient sediments: incompletely mineralized and patchily distributed.

ACKNOWLEDGMENTS

We thank M.E. Collinson, D. Edwards, D. Rickard, S.T. Grimes, I.B. Butler, and R. Raiswell for insights on pyritization, particularly of fossil plants. The experimental work was done when all three authors were at the Department of Earth Sciences, University of Bristol. This study was funded by Natural Environment Research Council grant GR3/11196.

REFERENCES

Allen, R.E., 2002, Role of diffusion-precipitation reactions in authigenic pyritization: Chemical Geology, v. 182, p. 461–472.

Allen, R.E., and Parkes, R.J., 1995, Digestion procedures for determining reduced sulfur species in bacterial cultures and in ancient and recent sediments, *in* Schoonen, V., ed., Geochemical Transformations of Sedimentary Sulfur: Washington, D.C., American Chemical Society, p. 243–257.

Aller, R.C., 1980, Quantifying solute distributions in the bioturbated zone of marine sediments by defining an average microenvironment: Geochimica et Cosmochimica Acta, v. 44, p. 1,955–1,965.

Allison, P.A., 1988, Taphonomy of the Eocene London Clay biota: Palaeontology, v. 31, p. 1,079–1,100.

Bartels, C., Briggs, D.E.G., and Brassel, G., 1998, The Fossils of the Hünsrück Slate: Marine Life in the Devonian: Cambridge, U.K., Cambridge University Press, 309 p.

Benning, L.G., Wilkin, R.T., and Barnes, H.L., 2000, Reaction pathways in the Fe-S system below 100°C: Chemical Geology, v. 167, p. 25–51.

Berner, R.A., 1969, The synthesis of framboidal pyrite: Economic Geology, v. 64, p. 383–384.

Berner, R.A., 1970, Sedimentary pyrite formation: American Journal of Science, v. 268, p. 1–23.

Berner, R.A., 1984, Sedimentary pyrite formation: An update: Geochimica et Cosmochimica Acta, v. 48, p. 605–615.

Bowerbank, J.S., 1840, A history of the fossil fruits and seeds of the London Clay: London, John Van Vorst.

Briggs, D.E.G., 1995, Experimental taphonomy: Palaios, v. 10, p. 539–550.

Briggs, D.E.G., 2003, The role of decay and mineralization in the preservation of soft-bodied fossils: Annual Review of Earth and Planetary Sciences, v. 31, p. 275–301.

Briggs, D.E.G., Bottrell, S.H., and Raiswell, R., 1991, Pyritization of soft-bodied fossils: Beecher's Trilobite Bed, Upper Ordovician, New York State: Geology, v. 19, p. 1221–1224.

Briggs, D.E.G., Raiswell, R., Bottrell, S.H., Hatfield, D., and Bartels, C., 1996, Controls on the pyritization of exceptionally preserved fossils: An analysis of the Lower Devonian Hünsrück Slate of Germany: American Journal of Science, v. 296, p. 633–663.

Butler, I.B., and Rickard, D., 2000, Framboidal pyrite formation via the oxidation of iron (II) monosulphide by hydrogen sulphide: Geochimica et Cosmochimica Acta, v. 64, p. 2,665–2,672.

Canfield, D.E., 1989a, Reactive iron in marine sediments: Geochimica et Cosmochimica Acta, v. 53, p. 619–632.

Canfield, D.E., 1989b, Sulfate reduction and oxic respiration in marine sediments: Implications for organic carbon preservation in euxinic environments: Deep-Sea Research, v. 36, p. 121–138.

Canfield, D.E., and Raiswell, R., 1991, Pyrite formation and fossil preservation, *in* Allison, P.A., and Briggs, D.E.G., eds., Taphonomy: Releasing the Data Locked in the Fossil Record: New York, Plenum Press, p. 337–387.

Canfield, D.E., Raiswell, R., and Bottrell, S.H., 1992, The reactivity of sedimentary iron minerals toward sulfide: American Journal of Science, v. 292, p. 659–683.

Chandler, M.E.J., 1964, The Lower Tertiary floras of southern England. IV. A survey of findings in the light of recent botanical observations: British Museum (Natural History), London. 151 p.

Cline, J.D., 1969, Spectrophotometric determination of hydrogen sulphide in natural waters: Limnology and Oceanography, v. 14, p. 454–458.

Collinson, M.E., 1983, Fossil Plants of the London Clay: London, Palaeontological Association, 121 p.

Conway Morris, S., 1986, The community structure of the Middle Cambrian Phyllopod Bed (Burgess Shale): Palaeontology, v. 29, p. 423–467.

Donald, R., and Southam, G., 1999, Low temperature anaerobic bacterial diagenesis of ferrous monosulphide to pyrite: Geochimica et Cosmochimica Acta, v. 63, p. 2,019–2,023.

Drobner, E., Huber, H., Wachtershauser, G., Rose, D., and Stetter, K.O., 1990, Pyrite formation linked with hydrogen evolution under anaerobic conditions: Nature, v. 346, p. 742–744.

Dunn, K.A., McLean, R.J.C., Upchurch G.R., Jr., and Folk, R.L., 1997, Enhancement of leaf fossilization potential by bacterial biofilms: Geology, v. 25, p. 1,119–1,122.

Ferguson, D.K., 1985, The origin of leaf assemblages—New light on an old problem: Review of Palaeobotany and Palynology, v. 46, p. 117–188.

Friedmann, W.E., and Cook, M.E., 2000, The origin and early evolution of tracheids in vascular plants: Integration of palaeobotanical and neobotanical data: Philosophical Transactions of the Royal Society, Series B, v. 355, p. 857–868.

Gabbott, S.E., Hou, X.-G., Norry, M.J., and Siveter, D.J., 2004, Preservation of Early Cambrian animals of the Chengjiang biota: Geology, v. 32, p. 901–904.

Giblin, A.E., and Howarth, R.W., 1984, Porewater evidence for a dynamic sedimentary iron cycle: Limnology and Oceanography, v. 29, p. 47–63.

Grimes, S.T., Brock, F., Rickard, D., Davies, K.L., Edwards, D., Briggs, D.E.G., and Parkes, R.J., 2001, Understanding fossilization: Experimental pyritization of plants: Geology, v. 29, p. 123–126.

Grimes, S.T., Davies, K.L., Butler, I.B., Brock, F., Edwards, D., Rickard, D., Briggs, D.E.G., and Parkes, R.J., 2002, Fossil plants from the Eocene London Clay: The use of pyrite textures to determine the mechanism of pyritization: Journal of the Geological Society, London, v. 159, p. 493–501.

Gupta, N.S., Collinson, M.E., Briggs, D.E.G., Evershed, R.P., and Pancost, R.D., 2006, Re-investigation of the occurrence of cutan in plants: Implications for the leaf fossil record: Paleobiology, v. 32, in press.

Kaplan, I.R., Emmery, K.O., and Rittenberg, S.C., 1963, The distribution and isotopic abundance of sulfur on recent marine sediments of southern California: Geochimica et Cosmochimica Acta, v. 27, p. 297–331.

Kenrick, P., and Edwards, D., 1988, The anatomy of Lower Devonian *Gosslingia breconensis* Heard based on pyritized axes, with some comments on the permineralization process: Botanical Journal of the Linnean Society, v. 97, p. 95–123.

Kenrick, P., Edwards, D., and Dales, R.C., 1991, Novel ultrastructure in water-conducting cells of the lower Devonian plant *Sennicaulis hippocrepiformis*: Palaeontology, v. 34, p. 751–766.

Lovley, D.R., and Chapelle, F.H., 1995, Deep subsurface microbial processes: Reviews of Geophysics, v. 33, p. 365–381.

Lovley, D.R., and Phillips, E.J.P., 1986a, Availability of ferric iron for microbial reduction in bottom sediments of the freshwater tidal Potomac River: Applied and Environmental Microbiology, v. 52, p. 7,511–7,517.

Lovley, D.R., and Phillips, E.J.P., 1986b, Organic matter mineralization with reduction of ferric iron in anaerobic sediments: Applied and Environmental Microbiology, v. 52, p. 683–689.

Luther, G.W., III, 1991, Pyrite synthesis via polysulfide compounds: Geochimica et Cosmochimica Acta, v. 55, p. 2,839–2,849.

Martin, D., Briggs, D.E.G., and Parkes, R.J., 2003, Experimental mineralization of invertebrate eggs and the preservation of Neoproterozoic embryos: Geology, v. 31, p. 39–42.

Poole, I., 1992, Pyritized twigs from the London Clay, Eocene, of Great Britain: Tertiary Research, v. 13, p. 71–85.

Poole, I., Davies, K.L., and Wilkinson, H.P., 2002, A review of the platanaceous

woods from the Eocene paratropical rainforest of south-east England: Botanical Journal of the Linnean Society, v. 139, p. 181–191.

RAISWELL, R., 1993, Kinetic controls on depth variations in localised pyrite formation: Chemical Geology, v. 107, p. 467–469.

RAISWELL, R., WHALER, K., DEAN, S., COLEMAN, M.L., and BRIGGS, D.E.G., 1993, A simple three-dimensional model of diffusion-with-precipitation applied to localised pyrite formation in framboids, fossils and detrital iron minerals: Marine Geology, v. 113, p. 89–100.

RAISWELL, R., and CANFIELD, D.E., 1988, Sources of iron for pyrite formation in marine sediments: American Journal of Science, v. 298, p. 219–245.

REID, E.M., and CHANDLER, M.E.J., 1933, The flora of the London Clay: London, British Museum (Natural History), vii + 561 p.

RICKARD, D., 1994, A new sedimentary pyrite formation model: Mineralogical Magazine, v. 58a, p. 772–773.

RICKARD, D., 1997, Kinetics of pyrite formation by the H_2S oxidation of iron (II) monosulfide in aqueous solutions between 25 and 125°C: The rate equation: Geochimica et Cosmochimica Acta, v. 61, p. 115–134.

RICKARD, D., and LUTHER, G.W., III, 1997, Kinetics of pyrite formation by the H_2S oxidation of iron (II) monosulfide in aqueous solutions between 25 and 125°C: The mechanism: Geochimica et Cosmochimica Acta, v. 61, p. 135–147.

SAGEMANN, J., BALE, S.J., BRIGGS, D.E.G., and PARKES, R.J., 1999, Controls on the formation of authigenic minerals in association with decaying organic matter: An experimental approach: Geochimica et Cosmochimica Acta, v. 63, p. 1,083–1,095.

SCHOONEN, M.A.A., and BARNES, H.L., 1991a, Reactions forming pyrite and marcasite from solution: I. Nucleation of FeS_2 below 100°C: Geochimica et Cosmochimica Acta, v. 55, p. 1495–1504.

SCHOONEN, M.A.A., and BARNES, H.L., 1991b, Reactions forming pyrite and marcasite from solution: II. Via precursors below 100°C: Geochimica et Cosmochimica Acta, v. 55, p. 1,505–1,514.

SCHOPF, J.M., 1975, Modes of fossil preservation: Review of Palaeobotany and Playnology, v. 20, p. 27–53.

SCOTT, A.C., 1990, Anatomical preservation of fossil plants, *in* Briggs, D.E.G., and Crowther, P.R., eds., Palaeobiology: A Synthesis: Oxford, U.K., Blackwell Science, p. 263–266.

SØRENSEN, J, 1982, Reduction of ferric iron in anaerobic, marine sediment and interaction with reduction of nitrate and sulfate: Applied Environmental Microbiology, v. 43, p. 319–324.

SPICER, R.A., 1991, Plant taphonomic processes, *in* Allison, P.A., and Briggs, D.E.G., eds., Taphonomy: Releasing the Data Locked in the Fossil Record: New York, Plenum Press, p. 71–113.

STOOKEY, L.L., 1970, Ferrozine—A new spectrophotometric reagent for iron: Analytical Chemistry, v. 42, p. 779–781.

STUMM, W., and MORGAN, J.J., 1981, Aquatic Chemistry, 2nd ed.: New York, Wiley Interscience, 780 p.

WIDDEL, F., and BAK, F., 1992, Gram-negative mesophilic sulfate-reducing bacteria, *in* Balows, A., Trüper, H.G., Dworkin, M., Harder, W., and Schleifer, K.H., eds., The Prokaryotes: New York, Springer-Verlag, p. 3,352–3,378.

WILBY, P.R., BRIGGS, D.E.G., and RIOU, B., 1996, Mineralisation of soft-bodied invertebrates in a Jurassic metalliferous deposit: Geology, v. 24, p. 847–850

WILKIN, R.T., and BARNES, H.L., 1996, Pyrite formation by reactions of iron monosulfides with dissolved inorganic and organic sulfur species: Geochimica et Cosmochimica Acta, v. 60, p. 4,167–4,179.

ACCEPTED APRIL 4, 2006